NANOSYSTEMS:
PHYSICS, CHEMISTRY, MATHEMATICS

Semenov K.N., et al. *Nanosystems: Phys. Chem. Math.*, 2024, **15** (6), 921–935.
http://nanojournal.ifmo.ru
DOI 10.17586/2220-8054-2024-15-6-921-935

Original article

Biomedical applications of graphene-based nanomaterials in gene delivery, tissue engineering, biosensing and for the development antibacterial agents

Konstantin N. Semenov[1,2,3], Sergei V. Ageev[1,2], Olga S. Shemchuk[1,3], Gleb O. Iurev[1,3], Abdelsattar O. E. Abdelhalim[4], Igor V. Murin[2], Pavel K. Kozhukhov[1], Anastasia V. Penkova[2], Dmitriy N. Maystrenko[3], Oleg E. Molchanov[3], Vladimir V. Sharoyko[1,2,3]

[1]Pavlov First St. Petersburg State Medical University, St. Petersburg, Russia

[2]St. Petersburg State University, St. Petersburg, Russia

[3]A. M. Granov Russian Research Centre for Radiology and Surgical Technologies, St. Petersburg, Russia

[4]Environmental Research Department, National Centre for Social and Criminological Research (NCSCR), Giza, Egypt

Corresponding author: Konstantin N. Semenov, knsemenov@gmail.com; Vladimir V. Sharoyko, sharoyko@gmail.com

PACS 87.85.Qr, 87.85.Rs

ABSTRACT Graphene and graphene oxide have emerged as promising materials in various biomedical applications due to their unique physicochemical properties. This review provides a comprehensive overview of their utilization in gene delivery, tissue engineering, biosensors and antibacterial and antimicrobial agents. In gene delivery, graphene-based materials offer efficient delivery platforms with enhanced cellular uptake and minimal cytotoxicity, promising advancements in gene therapy. Additionally, in tissue engineering, graphene and graphene oxide scaffolds exhibit excellent biocompatibility, electrical conductivity, and mechanical properties, facilitating cell adhesion, proliferation, and differentiation for tissue regeneration. Moreover, graphene-based biosensors demonstrate high sensitivity, selectivity, and stability, enabling rapid and accurate detection of biomolecules for diagnostic and therapeutic purposes. This review highlights the recent advancements, challenges, and future prospects of graphene and graphene oxide in revolutionizing biomedical technologies, paving the way for innovative solutions in healthcare.

KEYWORDS graphene, graphene oxide, composites, nanostructures, biocompatibility, biomedical applications

ACKNOWLEDGEMENTS The authors acknowledge St. Petersburg State University for a research project 11602266.

FOR CITATION Semenov K.N., Ageev S.V., Shemchuk O.S., Iurev G.O., Abdelhalim A.O.E., Murin I.V., Kozhukhov P.K., Penkova A.V., Maystrenko D.N., Molchanov O.E., Sharoyko V.V. Biomedical applications of graphene-based nanomaterials in gene delivery, tissue engineering, biosensing and for the development antibacterial agents. *Nanosystems: Phys. Chem. Math.*, 2024, **15** (6), 921–935.

Abbreviations

A549 – hypotriploid human alveolar basal epithelial cell line; AA – alginic acid; ADR – Adriamycin; AgNP – silver nanoparticle; anti-miR-21 – miRNA against miR-21; APTES – (3-aminopropyl)triethoxysilane; ATP – adenosine triphosphate; AuNP – gold nanoparticles; BPEI – branched polyethyleneimine; C2C12 – immortalized mouse myoblast cell line; CS – chitosan; DOX – doxorubicin; EGFP – enhanced green fluorescent protein; FA – folic acid; FAM – fluorescein amidite; GAP43 – growth associated protein 43; GBN – graphene-based nanomaterials; GFP – green fluorescent protein; GO – graphene oxide; GO–AgNP – conjugate of GO and silver nanoparticles; GONS – chemically synthesized graphene oxide nanosheet; GO–TCP/AA – nanocomposite based on GO, TCP and AA; ITO – indium tin oxide; HA – hydroxyapatite; HDAC1 – histone deacetylase 1; HEK293 – human embryonic kidney epithelial-like cell line; HepG2 – hepatocellular carcinoma cell line; HL-60 – human leukemia cell line; HRP – horseradish peroxidase; K-Ras – protein from Kirsten rat sarcoma encoded by KRAS proto-oncogene; MC3T3-E1 – osteoblastic cell line; MCF-7 – human breast adenocarcinoma cell line; MSC – mesenchymal stem cells; NIR – near-infrared light; NSC – neuronal stem cells; OPF – oligo(poly(ethylene glycol) fumarate; PAA – polyacrylic acid; PAMAM – polyamidoamine; PLC – polycaprolactone; PLC–GO–Ag–Arg – nanocomposite based on GO, PLC, argentum nanoparticles and L-arginine; pDNA – DNA plasmid; PEDOT – poly(3,4-ethylenedioxythiophene); PEG – polyethylene glycol; PEI – polyethylenimine; PLC – phospholipase C; PPI – polypropylenimine; PTT – photothermal therapy; rBMSCs – rat bone marrow stem cells; rGO – reduced

graphene oxide; rGO–AgNP – composite based on rGO and argentum nanoparticles; ROS – reactive oxygen species; SF – silk fibroin; shRNA – small hairpin RNA; SiNPs – silica nanoparticles ; siRNA – small interfering RNA; Stat 3-siRNA – targeted small interfering RNA against signal transducer and activator of transcription 3; TCP – calcium orthophosphate; TMC – trimethyl chitosan; TuJ1 – neuron-specific class III beta-tubulin.

1. Introduction

The analysis of recent publications shows that interest in studying graphene-based materials (GBN) remains strong. This is due to their unique structure and physicochemical properties, as well as the wide range of possibilities for their practical applications in various fields, including medicine [1] (for the creation of targeted drug delivery systems [2], bioimaging [3], tissue engineering [4], biosensors [5], and new materials with antibacterial [6] and antiviral properties [7]). Traditionally, GBN includes graphene, graphene oxide (GO), reduced graphene oxide (rGO), and graphene quantum dots (GQD) (Fig. 1). Let us briefly describe GBN.

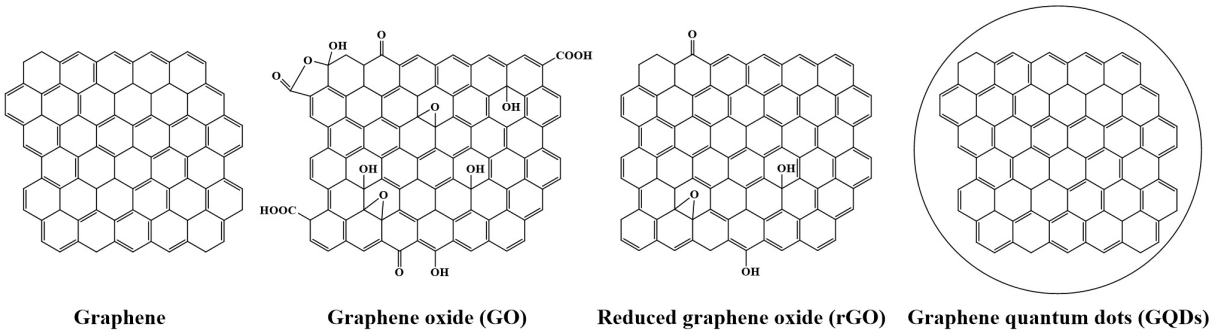

FIG. 1. Graphene-based materials

Graphene is two-dimensional material made of a single layer of carbon atoms arranged in a honeycomb lattice. Graphene was synthetized and characterized in 2004 by Andre Geim and Konstantin Novoselov. Due to the fact that carbon atoms in graphene are linked by both σ- and π- bonds, a very strong monoatomic structure with unique properties is formed. Graphene can be synthesized by chemical vapour deposition [8–14], electrochemical exfoliation [15–18] and mechanochemical exfoliation [19].

Graphene consisting oxygen-containing functional groups (epoxy, lactol, carboxyl, carbonyl, hydroxyl) [20, 21] in its structure called graphene oxide (GO) [21, 23, 24]. GO can be obtained by two main chemical methods: from nanosheets graphene and graphite [25]. The first method has not become widespread due to the complexity of the hardware and high costs: graphene sheets are oxidized in a vacuum chamber using atomic oxygen. In the second version of the synthesis, graphite is oxidized with strong oxidizing agents. This approach was a key to Hammers' [25], Brody [26] and Staudenmaier methods [27].

Reduced graphene oxide (rGO) is GBN, which is produced by reducing of GO using thermal and chemical reduction, for example by hydrazine hydrate, L-cysteine and other reducing agents [28–36]. rGO can been used as energy storage [37], as material for biomedical applications [38, 39] as well as in catalysis [40].

Graphene quantum dots (GQDs) are small, quasi-spherical graphene-based nanoparticles typically less than 10 nm in size. They can be used in bioimaging, drug delivery, sensors, and optoelectronics [41]. The following methods of obtaining of GQDs can be used: chemical synthesis [42–44], electron beam lithography [45], GO reduction [46, 47] and carbon nanotubes (CNTs) disintegration transformation [48]. In comparison with bulk graphene, GQDs offer the advantage of size-dependent properties due to quantum confinement and edge effects, which are absent in larger graphene sheets. This makes GQDs especially valuable in research areas focused on nanoscale phenomena, where precise control over material properties is crucial. Thus, while they share a common origin with graphene, GQDs stand out due to their unique properties that emerge specifically at the nanoscale, broadening the scope of applications for GBN.

In this review, we explore the recent advancements and challenges in utilizing graphene for gene delivery, tissue engineering, creation of biosensors and antibacterial and antimicrobial agents. By elucidating the underlying mechanisms and highlighting the promising outcomes, we aim to provide insights into the future directions of graphene-based technologies in biomedical research and clinical applications.

2. Gene delivery

Great interest of researchers in the field of nanobiomedicine is concentrated on the method of targeted correction of cell dysfunctions at the molecular genetic level. A key factor for the success of gene therapy is the development of delivery systems that can efficiently transport genetic material to the site of their therapeutic action without causing any associated side effects. Over the past ten years, much effort has been devoted to the creation of more efficient and biocompatible

vectors that can transfer nucleic acids into cells without inducing an immune response. There is an urgent need to develop a 'smart' nanocarrier, which can be loaded by various genetic materials, the carrier will transfer this material through various cellular structures without causing any immune response of the body and toxicity [49]. Currently, the Unified Register of Registered Medicines of the Eurasian Economic Union has not yet contained any nanoparticle drug for use in gene therapy. Thus, the development of optimal multifunctional nanoparticles for the delivery of genetic material is an urgent task [50, 51].

GO nanomaterials are suitable candidates for gene delivery due to their high loading rate and efficient gene transfection [52–56]. This has led to a number of research articles aimed at studying of covalent and non-covalent conjugates GO for gene delivery as shown in Table 1.

A number of studies have developed biomaterials for targeted delivery of axons and stimulation of the growth of transplanted neurons in the damaged spinal cord [64]. For this purpose, neuronal stem cells (NSCs) are used, which can differentiate into neurons and glial cells. Solanki *et al.* reported the creation of hybrid structures based on GO modified with silica nanoparticles (SiNPs) with immobilised NSCs. These hybrid structures (GO–SiNP) resulted in the formation of highly aligned axons from differentiating NSCs [65]. Immunocytochemical staining confirmed the presence of the neuronal marker TuJ1 and the axonal marker GAP43. In summary, the authors demonstrate the potential of using GO–SiNP as a novel hybrid material to enhance neuronal differentiation and axonal alignment, leading to accelerated functional recovery of injured spinal cord (Fig. 2).

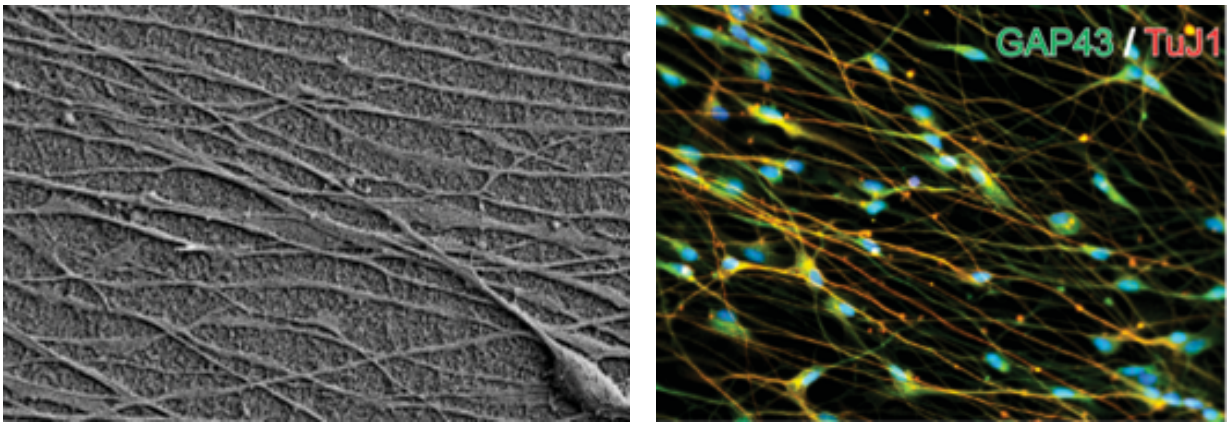

(a) (b)

FIG. 2. SEM image of GO–SiNP on a polydimethylsiloxane substrate showing highly aligned NSC axons at day 14 (*a*); immunocytochemistry results demonstrating the expression of the neuronal marker TuJ1 and the axonal marker GAP43 in NSCs (*b*) [65]

The success of gene therapy depends on the development of effective delivery systems for genetic material. Thus, the creation of biocompatible systems capable of transporting nucleic acids without side effects is a pressing issue. Nanomaterials such as GO are promising in this area due to their high loading capacity, gene transfection efficiency, and low toxicity.

3. Tissue engineering

Tissue engineering has become an important new field in medicine. A critical requirement in tissue engineering is the development of biomaterials that can mimic the biological environment and create a matrix for interaction with living cells, allowing cell attachment, proliferation and differentiation. GO-based materials have attracted attention due to their ease of functionalization coupled with high mechanical strength, stiffness, and electrical conductivity. One application of GO-based materials in tissue engineering is their use as reinforcements in hydrogels, films, fibres and fabrics to improve their physical and mechanical properties [66–73] (Table 2).

It has been shown that the creation of composite materials containing GBN leads to a significant improvement in physicochemical and mechanical properties, as well as biocompatibility, which collectively determines the promising potential of these materials in tissue engineering.

3.1. Tissue regeneration

Liu *et al.* [81] reported modification of GO with gelatine to biomimic charged proteins present in the ECM during bone formation. A GO–gelatine composite was used for biomimetic surface mineralisation with hydroxyapatite (HA). A detailed structural and morphological characterisation of the mineralised composite was carried out. In addition, the

TABLE 1. Modifications of graphene-based nanoplatforms for gene delivery systems

Characteristics of the conjugate	Effect	Ref.
GO conjugates with PEI, PPI), PAMAM and glycine, *N1*-(3-aminopropyl)butane-1.4-diamine	All conjugates showed significantly lower cellular toxicity compared to the individual polymer. The most successful effect was observed in the case of PEI conjugates, among which the most effective vector was the conjugate GO–PEI containing a glycine linker. This conjugate was nine times more effective in terms of the number of cells transfected with EGFP.	[55]
Conjugate based on GO modified with TMC and FA, for delivery of Survivin shRNA-expressing pDNA	Cytotoxicity of the conjugate was studied on HeLa cell line (cell survival after incubation for 24 h was 80 %) and A549 cell line (cell survival after incubation for 24 h is 98 %).	[56]
Non-covalent conjugate GO with PEI and PEG and Stat 3-siRNA	Results *in vivo* indicate significant regression of tumour growth and tumour weight after delivery of miRNA to block Stat3 using a plasmid supported by GO–PEI–PEG.	[57]
Non-covalent conjugate based on GO, modified with PEI and adriamycin (ADR), with miRNA against miR-21 (anti-miR-21)	Conjugate significantly enhanced the accumulation of ADR in MCF-7/ADR cells (an ADR-resistant mammary adenocarcinoma cell line) and exhibited much higher cytotoxicity than free ADR.	[58]
Non-covalent conjugate based on rGO modified with AuNP and PEI, with labelled FAM siRNA	The resulting composites allow efficient loading of siRNA, forming complexes for transport into HL-60 cells and suppressing the anti-apoptotic protein Bcl-2, which indicates that GBN conjugates are a suitable platform for gene delivery.	[59]
Non-covalent conjugates GO with grafted PEI and DNA plasmid against DNaseI; siRNA against GFP	Conjugate was used to sequentially deliver GFP-specific siRNA, resulting in $\sim$70 % suppression of target gene expression.	[60]
Non-covalent conjugate GO modified with PEI, PEG, chitosan-aconitic anhydride and chitosan-carballylic acid with shRNA (isolated from HepG2 cells) and DOX	The resulting systems effectively disrupted the endosome, significantly facilitating the release of DOX and shRNA into the cytoplasm. The systems demonstrated high efficiency of co-delivery of shRNA and DOX into HepG2 cell line.	[61]
Non-covalent conjugate based on GO, decorated with PEG and FA, and HDAC1 and K-Ras siRNAs targeting the HDAC1 gene and the mutant K-Ras gene, respectively	The synergistic combination of gene suppression and near-infrared PTT showed significant antitumour efficacy by inhibiting bulk tumour growth *in vivo* by more than 80 %.	[62]
GO conjugate with PEI, decorated with DNA plasmid and EGFP	The results demonstrate that GO is an effective platform for gene delivery, has low cytotoxicity, and may be promising in the field of virus-free gene therapy.	[63]

TABLE 2. GO containing nanocomposites used in tissue engineering

Application area	Characteristics of the conjugate	Effect	Ref.
Engineering and regeneration of cardiovascular tissue	Chitosan framework doped with GO nanoparticles decorated with AuNPs	The possibility of using a GO–AuNP nanocomposite as a reinforcing agent was demonstrated, which increased conduction velocity, contractility, and electrical circulation in the myocardium after infarction compared to individual chitosan	[74]
Engineering and regeneration of cardiovascular tissue	Adsorbed MSC on GO nanoparticles	MSC–GO implantation improved cardiac function, increased the number of engrafted MSCs and the amount of secreted paracrine factors that enhance angiogenesis and prevent further progression of myocardial infarction	[75]
Regeneration of skeletal muscles	Hybrid matrices based on a copolymer of lactic and glycolic acid and collagen, doped with GO	The introduction of composites increased the proliferation, differentiation and attachment of skeletal myoblasts of the C2C12 cell line	[76]
Regeneration of skeletal muscles	Composites based on PCL and GO	In cell viability experiments, the ratio levels and expression of genes encoding the myogenic markers CD56, myogenin and desmin were significantly increased with GO nanoparticles compared to control surfaces	[77]
Skin regeneration	PCL nanocomposite containing GO and AgNP nanoparticles decorated with l-arginine (Arg)	The PCL–GO–Ag–Arg conjugate showed biocompatibility with L929 mouse fibroblast cells. The composite exhibited proangiogenic effects on human endothelial cells	[78]
Bone tissue regeneration	Nanocomposite based on calcium orthophosphate (TCP) and alginic acid (AA) with the addition of GO	The cylindrical hybrid scaffolds were composed of GO–TCP/AA nanocomposite. The results showed that GO–TCP/AA scaffolds exhibited increased porosity, improved swelling profile, and better mechanical properties compared to TCP/AA	[79]
Creation of prostheses	GO nanosheet (GONS) and PAA/gelatine hydrogels	Tensile strength increased by 71 % and elongation at break increased by 26 % after adding 0.3 *wt.* % GONS	[80]

preosteoblast cell line MC3T3-E1 was cultured on the surface of GO–gelatine to visualise cellular activity and HA mineralisation. Higher cellular activities, namely cell adhesion, cell proliferation, and alkaline phosphatase activity, were observed on the GO–gelatine surface compared to the individual GO or glass surface. GO–gelatine composite promotes osteogenic differentiation of MC3T3-E1 cells. Moreover, the degree of surface mineralisation was studied using scanning electron microscopy (SEM) and alizarin red staining, and the formation of a native osteoid matrix was proven (Fig. 3). Taken together, the obtained data suggest that the GO–gelatine composite can be used as a scaffold material for osteogenesis and applied in orthopedic surgery.

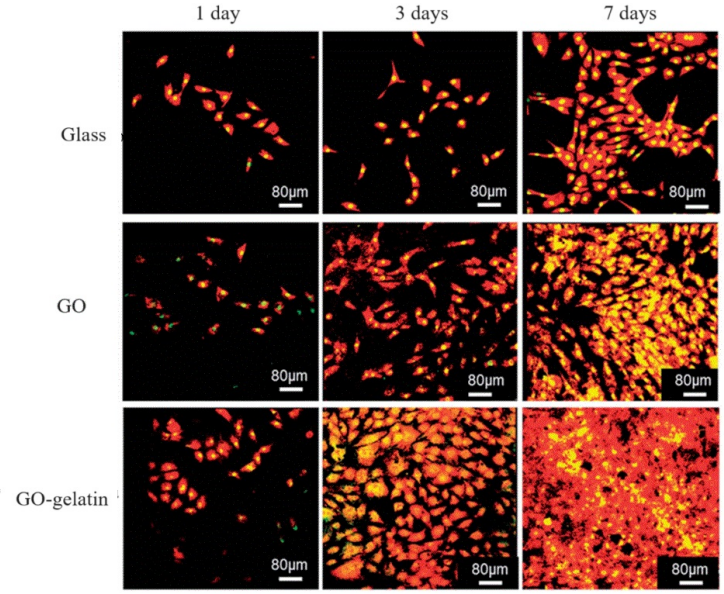

FIG. 3. Confocal fluorescence images of MC3T3-E1 cells cultured on glass, GO, and GO–gelatine composite for 1, 3, and 7 days [81]

Peng *et al.* [82] described a method for synthesizing a high-strength composite graphene hydrogel for bone tissue engineering. By combining GO, HA nanoparticles, and chitosan (CS) with crosslinking and reducing agents, researchers created a dense and oriented microstructure with improved mechanical strength, HA fixation capacity, and porosity. The study also highlights the importance of porosity and pore size for osteoblast proliferation and differentiation (porosity of nanomaterial was determined to be 84.37 %, the average pore size was 122 μm). Preliminary cell culture experiment using rat bone marrow stem cells (rBMSCs) demonstrated high viability and proliferation of osteoblasts on the composite hydrogel, suggesting its potential for use in bone tissue engineering applications.

The study [83] focuses on constructing a stem cell composite hydrogel scaffold for bone tissue engineering. Silk fibroin (SF) hydrogels were prepared with enzyme-catalyzed crosslinking, incorporating GO. The addition of GO resulted in more regular pore size and stable silk structure with excellent mechanical properties. Bone marrow stromal cells (BMSCs) encapsulated in the hydrogel showed enhanced growth, proliferation, and osteogenic differentiation, particularly at low GO concentrations. SEM revealed a porous structure conducive to cell proliferation and nutrient transport, with pore size influenced by GO content (addition of 0.05 % GO increases porosity by 2 %). Mechanical testing demonstrated improved anti-deformation ability and failure strain with the addition of GO. Osteogenic differentiation markers, such as alkaline phosphatase (ALP) and calcium nodules, increased significantly with SF/GO hydrogels, indicating promotion of osteogenesis. The SF/GO hydrogel exhibited excellent biocompatibility and potential for bone defect repair, highlighting its suitability for biomedical applications in bone tissue engineering.

The authors of [84] prepared a GO-based nanocomplex functionalized with polyethyleneglycol (PEG) and PEI for loading and delivering miR-29b, a key player in bone formation. The nanocomplex exhibited good biocompatibility, miR-29b loading capacity, and transfection efficiency. Encapsulating the miR-29b/GO-PEG-PEI nanocomplex into CS hydrogel for osteogenesis showed promising results *in vitro* and *in vivo*, promoting BMSC osteogenic differentiation and bone regeneration. The study suggests that PEG/PEI functionalized GO could serve as a promising candidate for miRNA cellular delivery, and the miR-29b/GO-PEG-PEI@CS hydrogel holds potential for repairing bone defects *in vivo*. Cytotoxicity testing revealed good biocompatibility of the GO-PEG-PEI complex, with efficient miRNA loading demonstrated through agarose gel electrophoresis and cellular uptake observed via laser scanning confocal microscopy. The transfection efficiency of miR-29b/GO-PEG-PEI varied with different mass ratio of nanoparticles to plasmid content (N/P), with the complex showing the highest transfection efficiency at an N/P ratio of 40. *In vivo* evaluation indicated increased bone formation in defects treated with miR-29b/GO-PEG-PEI@CS hydrogel compared to control groups, demonstrating its

potential for bone regeneration. Overall, the study suggests that the miR-29b/GO-PEG-PEI@CS hydrogel is a promising candidate for bone defect repair.

The studies presented show that GO-based composites with gelatin, hydrogels and other high-molecular compounds enhance cellular activity, making them promising for use in osteogenesis and orthopedic surgery. The presence of GO in composite materials improves mechanical properties, structural stability and porosity, which increases their suitability for bone tissue engineering.

3.2. Soft tissue regeneration

Graphene and its derivatives, have shown promise in promoting the growth of fibroblasts and keratinocytes, making them valuable in skin tissue engineering and wound healing. For instance, Khan *et al.* [85] developed a cost-effective composite hydrogel by crosslinking GO-functionalized arabinoxylan with polyvinyl alcohol (PVA), exhibiting improved antibacterial properties and biocompatibility, as well as efficacy in anticancer evaluations. Xue *et al.* [86] crafted a single-layer hydrogel artificial skin by incorporating dispersed peptide-coated graphene (PCG), resulting in a hydrogel with remarkable stretchability, mechanical sensing capabilities, and rapid self-healing abilities. Zhao *et al*. [87] designed a flexible hydrogel dressing for wound care, offering effective antibacterial properties through a photothermal mechanism. Additionally, conductive hydrogel design must consider both mechanical strength and electrical activity to mimic ECM properties. Zhou *et al.* [88] investigated the integration of GO into oligo(poly(ethylene glycol) fumarate) (OPF) hydrogels to enhance mechanical support and improve cellular electrical signaling, showing promise in myocardial infarction treatment. Yuan *et al.* [89] engineered a self-healing hydrogel within a silk protein (SP) framework, incorporating GO and growth factors for regenerative treatment in myocardial infarction therapy. Moreover, a novel injectable gel composed of rGO and alginate was created to transport mesenchymal stem cells, fostering the regeneration of injured cardiac tissue following a heart attack and supporting the viability and maturation of cardiac myocytes. These advancements hold significant potential in addressing complex tissue interactions and managing emergencies related to hemostasis outside the body.

As can be seen from the presented studies, functionalized graphene improves antibacterial properties and biocompatibility, as it promotes skin cell growth and wound healing; graphene-based hydrogels exhibit stretchability, self-healing ability, and are applicable for wound care. These materials can maintain mechanical strength, which can be used in the treatment of cardiovascular diseases such as myocardial infarction. These developments open up new possibilities in regenerative medicine and bleeding management.

4. Antimicrobial agents

Resistance of pathogenic bacteria to antibiotics has become a serious health care problem throughout the world, so replacing existing antibacterial agents is an urgent problem in material science [90, 91]. GBN have been intensively studied due to their antibacterial activity towards a wide range of bacteria [38, 92–95].

Metal composites containing graphene or GO have improved bactericidal properties than pure metal surfaces. In the composite, GO serves as an electron acceptor and captures electrons from the bacterial cell wall, and then transfers them to the metal substrate and thereby generates ROS production. This interrupts mitochondrial electron transport and ATP production in the bacterial cell, inhibiting its growth and viability [96].

Abdollahzadeh *et al.* carried out the synthesis of a metal-organic framework nanocomposite based on CS and GO. The resulting material has a high level of antibacterial activity with a maximum concentration of 2000 μg/mL. The studies were carried out using the disk diffusion method on Mueller–Hinton agar medium on bacteria of the species *Staphylococcus aureus* and *Escherichia coli* [97].

Bentedlaouti *et al.* prepared nanomaterials based on GO and rGO decorated with silver nanoparticles (AgNPs) [98]. Analysis of nanomaterials using SEM confirmed the intercalation of AgNPs into intermediate layers as nanosheets GO and rGO. Fig. 4 shows the results of a study of antibacterial activity using the paper disk method. The introduction of silver nanoparticles into tGO and trGO increased the antibacterial effect in relation to the individual GBN towards *Staphylococcus aureus* (by 2 – 3 times), *Bacillus cereus* (by 2 – 3 times), *Bacillus subtilis* (by 1.5 – 3 times), *Escherichia coli* (by 1.5 – 2 times), *Pseudomonas aeruginosa* (by 1.5 – 2 times) and *Candida albucans* (by 2.5 – 3 times).

A non-covalent nanocomposite based on GO and bimetallic Ag–Zr nanoparticles showed superior antibacterial and anti-biofilm activity of GO-decorated nanoparticles compared to bimetallic nanoparticles [99]. This effect may be due to the synergistic effect of the interaction between GO and Ag–Zr. This work showed a dose-dependent anti-biofilm activity of nanocomposites *in vitro* against biofilm-forming bacteria methicillin-resistant strain *Staphylococcus aureus* (MRSA). Ag–Zr nanoparticles inhibited 68.11 % and Ag–Zr/GO inhibited 71.12 % of MRSA biofilm formation (Fig. 5). MRSA biofilms were visualised using confocal scanning laser microscopy.

Nitrogen doped quantum carbon dots have been produced by hydrothermal synthesis [100]. The study of their antibacterial activity was determined using the minimum inhibitory concentration (MIC) test on *Bacillus subtilis* strain. The results showed no inhibition in carbon quantum dot samples without nitrogen, while samples containing 4.2 and 5 g of nitrogen had inhibitory activity at concentrations of 100 – 200 ppm. Moreover, the sample with the maximum nitrogen content demonstrated maximum activity [100].

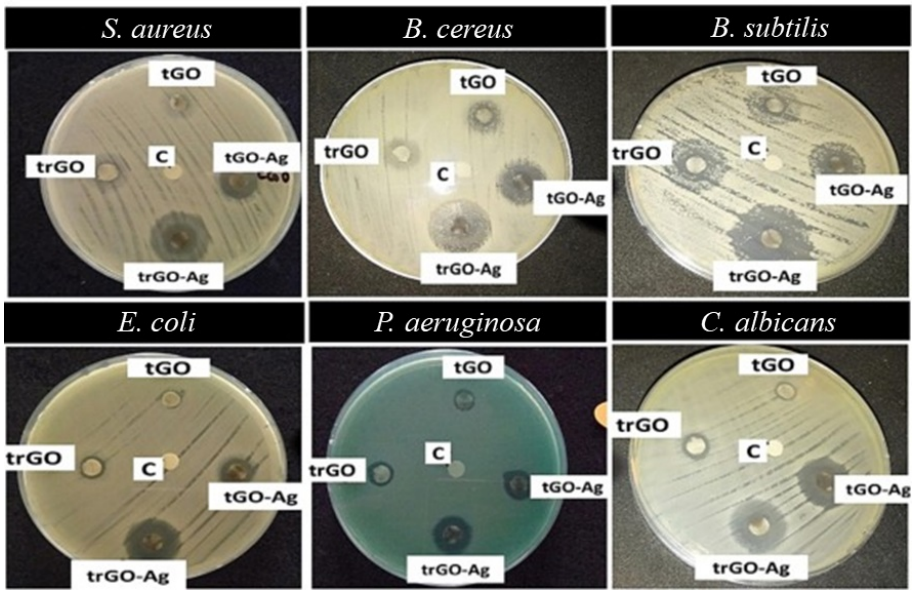

FIG. 4. Antibacterial test results using the paper disc diffusion method against microorganisms, (*c*) – control [98]. tGO and trGO are GO and rGO obtained by thermal synthesis, tGO-Ag and, trGO-Ag are GO and rGO obtained by thermal synthesis with silver nanoparticles

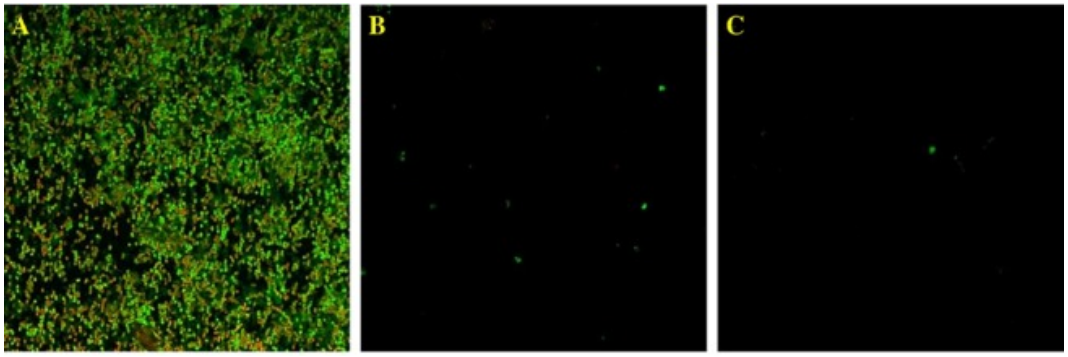

FIG. 5. Confocal images of anti-biofilm activity of nanoparticles. Control (*a*), bimetallic Ag–Zr NPs (*b*), Ag–Zr/GO nanocomposite (*c*) [99]

Hemmat *et al.* revealed that GO non-covalently functionalised with CuI using a hydrothermal method, the nanocomposite managed to inhibit the growth of gram-negative (*Escherichia coli*) and gram-positive (*Staphylococcus aureus*) bacteria. The mechanism of antibacterial activity was attributed to the oxidative stress due to generation of ROS, physical disruption, and wrapping of bacterial membranes owing to the GO sharp edges [101]. Metal oxide nanoparticles such as copper oxide were decorated on GO surface using ginger essential oil (GEO) as eco-friendly approach, the nanocomposite showed enhanced at about two times antibacterial activity against *Staphylococcus aureus* and *Escherichia coli* [102].

Metal nanoparticles such as copper nanopowders were incorporated with graphene surface, the nanocomposite exhibited strong antibacterial activity and achieved 99 % reduction of *Escherichia coli* bacteria within 1 h [103]. Yang *et al.* demonstrated that the antibacterial activity of medical titanium was strengthened through coating its surface by GO and copper, the GO–Cu–Ti has proved *in vitro* and *in vivo* antibacterial activity (over 99 %) against Staphylococcus aureus, and *Escherichia coli* bacteria due to synergistic effect of both GO and Cu, generation of ROS, and sharp-edged GO sheets that physically damage bacterial membranes [104]. Moreover, the functionalised graphene surface with aliphatic molecules such as diaminohexane was also activated using AgNPs for the antibacterial activity against total and faecal coliform bacteria [105]. Derakhshi *et al.* revealed that AgNPs were stabilised on rGO using dimethyl formamide (DMF), and the distributed AgNPs have different shapes depending on the synthesis method. The authors displayed that the shape of AgNPs formed on the amine functionalised rGO, have significant effect on the inhibition of bacterial growth, where triangular AgNPs exhibited highest antibacterial activity against both *Escherichia coli* and *Staphylococcus aureus* in comparison with the spherical AgNPs and silver nanowires [106].

The antibacterial activity was increased through the synergistic effect produced as a result of combining organic polymer of tetraethynyl porphyrin with GO surface for enhancing the antibacterial activity against gram-positive (*Staphylococcus aureus*) and gram-negative (*Escherichia coli*) pathogens in comparison with the free counterparts (the bare GO, and porphyrin), the synergistic effect could significantly accelerate the healing of open wound infected by bacteria [107].

Graphene–bismuth oxychloride 2D heterojunction killed *Staphylococcus aureus* bacteria with 99.36 % under simulated sunlight irradiation for 20 min, the antibacterial properties of heterojunction was attributed to graphene by 57.31 %. In the latter case graphene has the ability to transfer the excited electrons of BiOCl semiconductor exposed to visible light irradiation conjugated with the electrons on graphene surface for enhancing the photocatalytic antibacterial performance through surface plasmon resonance effect [108].

Sun *et al.* displayed that rGO was covalently attached to silanised titanium surface ((3-aminopropyl)triethoxysilane–titanium sheets) and showed high antibacterial activity against *Escherichia coli* and *Staphylococcus aureus* bacteria in comparison with titanium sheets, the SEM results of bacterial morphology illustrated that the dead bacteria were recorded on the graphene coated titanium more than the titanium sheets, the size and shape of both types of bacteria changed, the bacterial membranes were deformed and damaged. Levofloxacin antibiotic was noncovalently anchored on the graphene coated titanium through π–π stacking interaction, hydrogen bonds, and electrostatic interactions and proved inhibition for the abovementioned types of bacteria *in vivo* for the potential applications in oral implant surfaces for treatment of bacterial infection [109].

Thus, the growing resistance of bacteria to antibiotics requires the development of new antibacterial materials. GBN (GO, rGO) have shown effectiveness against various pathogens. Composites with graphene enhance bactericidal properties by suppressing bacterial activity due to the generation of ROS. The incorporation of metal nanoparticles, such as copper and silver, into graphene structures increases antibacterial activity, which can accelerate wound healing. These developments offer new approaches to combating infections, including application in medical implants.

5. Nanobiosensors

Nanobiosensors are nanomaterials that are applied in the field of biosensors for different applications such as diagnosis of diseases, viruses and bacteria, environmental monitoring, food industry, healthcare and clinical uses [110–115]. Different components contribute to the composition of a biosensor:

- blood, urine, saliva, bacteria, virus, fungi, water, food, soil, gases or air samples can serve as analytes;
- antibodies, enzymes, DNA, RNA, peptides, aptamers, organic molecules or metals and nanoparticles can act as a recognition element or bioreceptor;
- the transducer part is responsible for the transferring of the signal to the detector when exposed to any change happening on its surface such as chemical redox reactions, or physical changes. Carbon nanomaterials are widely used as transducers due to their high surface area, special electronic, optical, thermal and mechanical properties;
- the detector can translate the electrical signal received from the transducer to quantitative and qualitative data [116].

The nanobiosensors are divided into electrochemical, optical calorimetric and piezoelectric:

- electrochemical nanobiosensors are based on transducing the biochemical signals to electrical ones [117];
- optical nanobiosensors are based on the interaction between analyte and sensor which leads to a change in the morphology and fluorescence of the transducer under irradiation. The optical sensing can be achieved through Raman scattering, fluorescence, and plasmon resonance [118];
- calorimetric nanobiosensors are based on the detection of the heat liberated or consumed by a reaction between the analyte and the bioreceptor on the transducer surface [119];
- in case of piezoelectric nanobiosensors, the mechanical force produced due to the conjugation of the analyte with the sensor is transferred into electrical signal by the transducer and recognised by the detector [120].

Hernández *et al.* demonstrated that DNA aptamers were covalently and non-covalently attached to GBN (GO and rGO) as the transducer surfaces for the detection of living organisms such as *Staphylococcus aureus* with high selectivity detecting even single CFU/mL of the bacteria [121]. Electrochemical biosensor was developed from graphene functionalised with black phosphorus and gold nanoparticles for the detection of sortase enzyme which can catalyse the covalent attachment of surface proteins to the cell walls of gram-positive bacteria. A linear dynamic range was obtained between 1 pM – 100 nM with LOD of 0.65 pM, compared to the fluorimetric method, where linear range was 300 pmol/L – 100 nmol/L and LOD was 0.16 nM [122].

Yang *et al.* demonstrated that the biosensors fabricated from rGO modified with poly(methylene blue) and poly(ionic liquids) were applied in detecting SARS-CoV2-spike protein in clinical serum samples for the diagnosis and treatment of COVID-19, with a detection range of 0.1$\sim$1000 ng/mL and LOD 38 pg/mL, compared to AuNPs/carbon cloth nanomaterial with linear range 0 $\sim$ 1000 ng/mL and LOD 110 pg/mL [123]. Field effect transistor biosensor based on GO was applied to detect SARS-CoV2 spike protein. Sheets of GO were π–π stacked to the graphene surface and formed Van der Waals heterostructure, the antibody was immobilised on the GO surface providing high affinity to interact with the protein with LOD around 8 fg/mLwith detection range between 10 fg/mL to 100 pg/mL, which showed enhancement of sensitivity in three times compared to biosensor based on graphene field effect transistor [124]. A genosensor was

developed by Malla *et al.* where rGO was modified by gold nanoparticles and covalently functionalised with DNA probes for targeting the SARS-CoV2 gene efficiently in human saliva, urine, and serum with LOD 0.37, 0.33, and 0.19 fM, respectively, compared to gold electrode with LOD 26 fM [125].

Laser scribed graphene modified with gold nanoparticles and molecularly imprinted polymer was developed to detect the human epidermal growth factor receptor 2 (HER2) protein, a biomarker for breast cancer. Detection of HER2 was performed in the concentration range from 1 to 200 ng/mL with a LOD of 0.43 ng/mL, leading to early diagnosis of breast cancer [126]. Chemiresistive biosensors were fabricated from crumpled graphene modified by polystyrene as a heat shrinkable material. The DNA was covalently immobilised on GO surface through amide bond formation for the purpose of targeting miRNA-21; the rate of changing electrical resistance was measured when the target miRNA-21 interacts with GO surface. A linear change occurs with increasing the concentration of miRNA-21 from 10 nM to 1 pM with LOD of 1.47 pM, revealing the high sensitivity and selectivity of the biosensor for cancer biomarkers [127]. Yan *et al.* developed the electrochemical aptasensor from graphene nanosheets modified with AgNPs and thiolated aptamer for the detection of the carcinoembryonic antigen with high selectivity, reproducibility, and sensitivity proved in a wide linear range from 0.001 to 10 pg/mL with LOD of 0.5 fg/mL, compared to $Ag/MoS_2@Fe_3O_4$ with linear range 0.1 – 20000 pg/mL and LOD 0.03 pg/mL, applied in human serum samples [128].

Rajaji *et al.* showed that an electrochemical nanosensor was efficiently prepared from rGO decorated with iron nitride nanoparticles immobilised on carbon electrode for the rapid detection of the cancer biomarker of 4-nitroquinoline *N*-oxide; the fabricated nanosensor showed a wide range of detection from 0.05 – 574.2 μM and LOD of 9.24 nM, the nanosensor was applied for analysis in human blood and urine samples [129].

Rauf *et al.* developed an electrochemical immunosensor based on GO enriched with carboxylic groups covalently modified with antibody against the cancer biomarker mucin-1. The immunosensor was fabricated on screen-printed carbon electrodes and showed high sensitivity with linear range of detection from 0.1 to 2 U/mL with LOD of 0.04 U/mL in human serum samples, compared to coated PMMA beads with linear range 0.3 – 20 U/mL and LOD 0.21 U/mL. At the electrode surface, methylene blue probe was redox catalysed by the active nanosensor and reduced to a leucomethylene blue as an indicator for detection of antibody-protein interactions [130].

Kumar *et al.* constructed a nanosensor from yttria-doped zirconia-reduced GO nanocomposite that was functionalised with 3-(triethoxysilyl)propan-1-amine. The nanocomposite was then electrophoretically deposited onto an electrode of indium tin oxide coated glass substrate. CYFRA-21-1 antibody cancer biomarker were then covalently immobilised on the nanocomposite surface. The obtained nanobiosensor proved highly sensitive detection for the salivary cancer biomarker CYFRA-21-1 with linear detection range from 0.01 – 50 ng/mL with LOD of 7.2 pg/mL, compared to $APTES/nHfO_2/ITO$ nanoparticles with linear range 2 – 18 ng/mL and LOD 0.21 ng/mL [131].

Singh *et al.* deposited layers of graphene sheets on copper substrate through chemical vapour deposition technique with subsequent non-covalent functionalisation with 1-pyrenebutanoic acid succinimidyl ester through π–π stacking interaction followed by covalent functionalisation with the antibody for the detection of the cancer biomarker carcinoembryonic antigen (CEA). The constructed biosensor approved high sensitivity and selectivity with linear detection range from 1.0 to 25.0 ng/mL and LOD of 0.23 ng/mL, compared to complex material of HRP, AuNPs, Carboxylic magnetic beads, graphene, hexacyanoferrates and SiO_2 with linear range 5 – 60 ng/mL and LOD 5 ng/mL [132].

Sadeghi *et al.* fabricated aptasensor based on electrochemically synthesised GO layers on graphite electrode and covalently conjugated through amide bonds with aptamers that are specific to the HER2. The nanobiosensor confirmed the ability for early diagnosis of breast cancer, high sensitivity and selectivity with a linear detection range from 0.5 to 25 ng/mL with LOD of 0.59 ng/mL [133].

The GBN can also be used in the diagnosis of neurodegenerative diseases such as Alzheimer's and Parkinson's. Chen *et al.* developed an electrochemical sensor from the nanocomposite based on rGO and manganese sulphide nanoparticles. The authors revealed high selectivity and sensitivity towards Parkinson's disease biomarker (dopamine). The nanosensor demonstrated a wide linear range of detection of dopamine between 0.02 and 438.6 μM and LOD of 3.5 nM in human and rat serum, compared to PEDOT/Pd with linear range 0.5 – 1.0 μM and LOD 0.5 μM [134].

Nanobiosensors play an important role in disease diagnostics. They demonstrate high selectivity, for example, for detecting bacteria, viruses and cancer biomarkers. The use of graphene modified with various nanoparticles (gold, silver and others) allows creating effective electrochemical biosensors. These sensors are also promising in the diagnosis of neurodegenerative diseases with high accuracy and sensitivity.

6. Conclusion

GBN materials are of great benefit to modern science in particular due to their potential applications in medicine and bioengineering (Fig. 6). In this review it was shown that GBN can be effectively used for development of nanobiosensors, to deliver genetic material with minimal toxicity, as well as to improve the mechanical properties of biomaterials in tissue engineering. GBN composites promote bone tissue regeneration and can be applied in orthopedic surgery; GBN improves the antibacterial properties of materials, accelerating wound healing and suppressing pathogen activity, which is useful for medical implants.

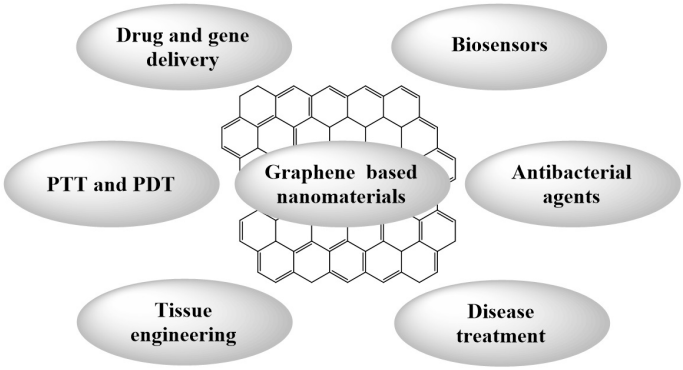

FIG. 6. Directions of GBN application in biomedicine

It is well known that one of the main problems of using nanomaterials in medicine is that their properties are determined not only by the chemical composition, but also by the variety of their surface characteristics and morphology, that implies the complexity their standardization. At present, detailed analysis of the literature data reveals the following problems in the field of GBN investigation: (*i*) lack of data on identification of the synthesized nanomaterial; (*ii*) non-sufficient reproducibility of GBN syntheses; (*iii*) lack of studies devoted to the stability of GBN dispersions; (*iv*) absence of data on the metabolic stability, mechanisms of action, signaling pathways and pharmaco- and toxicokinetics of GBN.

References

[1] Abdelhalim A.O.E., Semenov K.N., Nerukh D.A., Murin I V., Maistrenko D.N., Molchanov O.E., Sharoyko V.V. Functionalisation of graphene as a tool for developing nanomaterials with predefined properties. *J. Mol. Liq.*, 2022, **348**, 118368.

[2] Saharan R., Paliwal S.K., Tiwari A., Tiwari V., Singh R., Beniwal S.K., Dahiya P., Sagadevan S. Exploring graphene and its potential in delivery of drugs and biomolecules. *J. Drug. Deliv. Sci. Technol.*, 2023, **84**, 104446.

[3] Lin J., Huang Y., Huang P. Graphene-Based Nanomaterials in Bioimaging, In *Biomedical Applications of Functionalized Nanomaterials: Concepts, Development and Clinical Translation*, 2018, Elsevier, P. 247–287.

[4] Cao Z., Bian Y., Hu T., Yang Y., Cui Z., Wang T., Yang S., Weng X., Liang R., Tan C. Recent advances in two-dimensional nanomaterials for bone tissue engineering. *J. of Materiomics*, 2023, **9** (5), P. 930–958.

[5] Prasad S.V.S., Kumar M., Arulananth T.S., Ravi B., Kumar B., Kiran Kumar B. Graphene/ZnO nanocomposite based optical biosensors. *Mater Today Proc*, 2023.

[6] Kumar P., Huo P., Zhang R., Liu B. Antibacterial Properties of Graphene-Based Nanomaterials. *Nanomaterials*, 2019, **9** (5), 737.

[7] Palmieri V., Papi M. Can graphene take part in the fight against COVID-19? *Nano Today*, 2020, **33**, 100883.

[8] Zhang Y., Zhang L., Zhou C. Review of chemical vapor deposition of graphene and related applications. *Acc. Chem. Res.*, 2013, **46** (10), P. 2329–2339.

[9] Muñoz R., Gómez-Aleixandre C. Review of CVD synthesis of graphene. *Chemical Vapor Deposition*, 2013, **19** (10–12), P. 297–322.

[10] Li X., Colombo L., Ruoff R.S. Synthesis of Graphene Films on Copper Foils by Chemical Vapor Deposition. *Advanced Materials*, 2016, **28** (29), P. 6247–6252.

[11] Chen K., Shi L., Zhang Y., Liu Z. Scalable chemical-vapour-deposition growth of three-dimensional graphene materials towards energy-related applications. *Chem. Soc. Rev.*, 2018, **47** (9), P. 3018–3036.

[12] Yang X., Zhang G., Prakash J., Chen Z., Gauthier M., Sun S. Chemical vapour deposition of graphene: layer control, the transfer process, characterisation, and related applications. *Int. Rev. Phys. Chem.*, 2019, **38** (2), P. 149–199.

[13] Mattevi C., Kim H., Chhowalla M. A review of chemical vapour deposition of graphene on copper. *J. Mater. Chem.*, 2011, **21** (10), P. 3324–3334.

[14] Zhou H., Yu W.J., Liu L., Cheng R., Chen Y., Huang X., Liu Y., Wang Y., Huang Y., Duan X. Chemical vapour deposition growth of large single crystals of monolayer and bilayer graphene. *Nat. Commun.*, 2013, **4** (1), P. 1–8.

[15] Yu P., Lowe S.E., Simon G.P., Zhong Y.L. Electrochemical exfoliation of graphite and production of functional graphene. *Curr. Opin. Colloid Interface Sci.*, 2015, **20** (5–6), P. 329–338.

[16] Rao K.S., Senthilnathan J., Liu Y.F., Yoshimura M. Role of peroxide ions in formation of graphene nanosheets by electrochemical exfoliation of graphite. *Sci. Rep.*, 2014, **4** (1),P. 1–6.

[17] Wan H., Wei C., Zhu K., Zhang Y., Gong C., Guo J., Zhang J., Yu L. Zhang J. Preparation of graphene sheets by electrochemical exfoliation of graphite in confined space and their application in transparent conductive films. *ACS Appl. Mater. Interfaces*, 2017, **9** (39), P. 34456–34466.

[18] Mir A., Shukla A. Bilayer-rich graphene suspension from electrochemical exfoliation of graphite. *Mater. Des.*, 2018, **156**, P. 62–70.

[19] Melezhik A.V., Pershin V.F., Memetov N.R. Tkachev A.G. Mechanochemical synthesis of graphene nanoplatelets from expanded graphite compound. *Nanotechnol. Russ.*, 2016, **11** (7–8), P. 421–429.

[20] Abdelhalim A.O.E., Semenov K.N., Nerukh D.A., Murin I. V., Maistrenko D.N., Molchanov O.E., Sharoyko V.V. Functionalisation of graphene as a tool for developing nanomaterials with predefined properties. *J. Mol. Liq.*, 2022, **348**, 118368.

[21] Abdelhalim A.O.E., Sharoyko V.V., Ageev S.V., Farafonov V.S., Nerukh D.A., Postnov V.N., Petrov A.V., Semenov K.N. Graphene Oxide of Extra High Oxidation: A Wafer for Loading Guest Molecules. *J. Phys. Chem. Lett.*, 2021, **12** (41), P. 10015–10024.

[22] Abdelhalim A.O.E., Meshcheriakov A.A., Maistrenko D.N., Molchanov O.E., Ageev S.V., Ivanova D.A., Iamalova N.R., Luttsev M.D., Vasina L.V., Sharoyko V.V., Semenov K.N. Graphene oxide enriched with oxygen-containing groups: on the way to an increase of antioxidant activity and biocompatibility. *Colloids Surf B Biointerfaces*, 2021, 112232.

[23] Taneva S.G., Krumova S., Bogár F., Kincses A., Stoichev S., Todinova S., Danailova A., Horváth J., Násztor Z., Kelemen L., Dér A. Insights into graphene oxide interaction with human serum albumin in isolated state and in blood plasma. *Int. J. Biol. Macromol.*, 2021, **175**, P. 19–29.

[24] Anirudhan T.S., Chithra Sekhar V., Athira V.S. Graphene oxide based functionalized chitosan polyelectrolyte nanocomposite for targeted and pH responsive drug delivery. *Int. J. Biol. Macromol.*, 2020, **150**, P. 468–479.
[25] Hummers W.S., Offeman R.E) Preparation of Graphitic Oxide. *J. Am. Chem. Soc.*, 1958, **80** (6), P. 1339–1339.
[26] Brodie B.C. On the atomic weight of graphite. *Philos. Trans. R. Soc. Lond.*, 1859, **149** (1859), P. 249–259.
[27] Staudenmaier L. Verfahren zur Darstellung der Graphitsäure. *Berichte der deutschen chemischen Gesellschaft*, 1898, **31** (2), P. 1481–1487.
[28] Abdelhalim A.O.E., Sharoyko V.V., Meshcheriakov A.A., Martynova S.D., Ageev S.V., Iurev G.O., Al Mulla H., Petrov A.V., Solovtsova I.L., Vasina L.V., Murin I.V., Semenov K.N. Reduction and functionalization of graphene oxide with L-cysteine: Synthesis, characterization and biocompatibility. *Nanomedicine*, 2020, **29**, 102284.
[29] Lavin-Lopez M.P., Paton-Carrero A., Sanchez-Silva L., Valverde J.L., Romero A. Influence of the reduction strategy in the synthesis of reduced graphene oxide. *Advanced Powder Technology*, 2017, **28** (12), P. 3195–3203.
[30] Guex L.G., Sacchi B., Peuvot K.F., Andersson R.L., Pourrahimi A.M., Ström V., Farris S., Olsson R.T. Experimental review: Chemical reduction of graphene oxide (GO) to reduced graphene oxide (rGO) by aqueous chemistry. *Nanoscale*, 2017, **9** (27), P. 9562–9571.
[31] De Silva K.K.H., Huang H.H., Joshi R.K., Yoshimura M. Chemical reduction of graphene oxide using green reductants. *Carbon N.Y.*, 2017, **119**, P. 190–199.
[32] Wang J., Salihi E.C., siller L. Green reduction of graphene oxide using alanine. *Materials Science and Engineering C*, 2017, **72**, P. 1–6.
[33] Alam S.N., Sharma N., Kumar L. Synthesis of Graphene Oxide (GO) by Modified Hummers Method and Its Thermal Reduction to Obtain Reduced Graphene Oxide (rGO)*. *Graphene*, 2017, **06** (01), P. 1–18.
[34] Saleem H., Haneef M., Abbasi H.Y. Synthesis route of reduced graphene oxide via thermal reduction of chemically exfoliated graphene oxide. *Mater. Chem. Phys.*, 2018, **204**, P. 1–7.
[35] Oliveira A.E.F., Braga G.B., Tarley C.R.T., Pereira A.C. Thermally reduced graphene oxide: synthesis, studies and characterization. *J. Mater. Sci.*, 2018, **53** (17), P. 12005–12015.
[36] Schedy A., Oetken M. The thermal reduction of graphene oxide – A simple and exciting manufacturing process of graphene. *CHEMKON*, 2020, **27** (5), P. 244–249.
[37] Liu Z., Navik R., Tan H., Xiang Q., Wahyudiono Goto M., Ibarra R.M., Zhao Y. Graphene-based materials prepared by supercritical fluid technology and its application in energy storage. *J. Supercrit. Fluids*, 2022, **188**, 105672.
[38] Mann R., Mitsidis D., Xie Z., McNeilly O., Ng Y.H., Amal R., Gunawan C. Antibacterial Activity of Reduced Graphene Oxide. *J. Nanomater.*, 2021, **2021**, P. 1–10.
[39] Robinson J.T., Perkins F.K., Snow E.S., Wei Z., Sheehan P.E. Reduced Graphene Oxide Molecular Sensors. *Nano Lett.*, 2008, **8** (10), P. 3137–3140.
[40] Dong N., Ye Q., Zhang D., Xiao Y., Dai H. Reduced graphene oxide as an effective promoter to the layered manganese oxide-supported Ag catalysts for the oxidation of ethyl acetate and carbon monoxide. *J. Hazard Mater.*, 2022, **431**, 128518.
[41] Zhao J., Tang L., Xiang J., Ji R., Yuan J., Zhao J., Yu R., Tai Y., Song L. Chlorine doped graphene quantum dots: Preparation, properties, and photovoltaic detectors. *Appl. Phys. Lett.*, 2014, **105** (11).
[42] Mueller M.L., Yan X., McGuire J.A., Li L. Triplet States and Electronic Relaxation in Photoexcited Graphene Quantum Dots. *Nano Lett.*, 2010, **10** (7), P. 2679–2682.
[43] Tang L., Ji R., Li X., Teng K.S., Lau S.P. Energy-level structure of nitrogen-doped graphene quantum dots. *J. Mater. Chem. C Mater.*, 2013, **1** (32), 4908.
[44] Peng J., Gao W., Gupta B.K., Liu Z., Romero-Aburto R., Ge L., Song L., Alemany L.B., Zhan X., Gao G., Vithayathil S.A., Kaipparettu B.A., Marti A.A., Hayashi T., Zhu J.-J., Ajayan P.M. Graphene Quantum Dots Derived from Carbon Fibers. *Nano Lett.*, 2012, **12** (2), P. 844–849.
[45] Ponomarenko L.A., Schedin F., Katsnelson M.I., Yang R., Hill E.W., Novoselov K.S., Geim A.K. Chaotic Dirac Billiard in Graphene Quantum Dots. *Science*, 2008, **320** (5874), P. 356–358.
[46] Shen J., Zhu Y., Yang X., Zong J., Zhang J., Li C. One-pot hydrothermal synthesis of graphenequantum dots surface-passivated by polyethylene glycol and their photoelectric conversion under near-infrared light. *New J. Chem.*, 2012, **36** (1), P. 97–101.
[47] Gupta V., Chaudhary N., Srivastava R., Sharma G.D., Bhardwaj R., Chand S. Luminscent Graphene Quantum Dots for Organic Photovoltaic Devices. *J. Am. Chem. Soc.*, 2011, **133** (26), P. 9960–9963.
[48] Lin L., Zhang S. Creating high yield water soluble luminescent graphene quantum dots via exfoliating and disintegrating carbon nanotubes and graphite flakes. *Chemical Communications*, 2012, **48** (82), 10177.
[49] Danaeifar M. Recent advances in gene therapy: genetic bullets to the root of the problem. *Clin. Exp. Med.*, 2022, **23** (4), P. 1107–1121.
[50] Wong J.K.L., Mohseni R., Hamidieh A.A., MacLaren R.E., Habib N., Seifalian A.M. Will Nanotechnology Bring New Hope for Gene Delivery? *Trends Biotechnol.*, 2017, **35** (5), P. 434–451.
[51] Yin H., Kanasty R.L., Eltoukhy A.A., Vegas A.J., Dorkin J.R., Anderson D.G. Non-viral vectors for gene-based therapy. *Nat. Rev. Genet.*, 2014, **15** (8), P. 541–555.
[52] Cao X., Zheng S., Zhang S., Wang Y., Yang X., Duan H., Huang Y., Chen Y. Functionalized Graphene Oxide with Hepatocyte Targeting as Anti-Tumor Drug and Gene Intracellular Transporters. *J. Nanosci. Nanotechnol.*, 2015, **15** (3), P. 2052–2059.
[53] Choi H.Y., Lee T.-J., Yang G.-M., Oh J., Won J., Han J., Jeong G.-J., Kim J., Kim J.-H., Kim B.-S., Cho S.-G. Efficient mRNA delivery with graphene oxide-polyethylenimine for generation of footprint-free human induced pluripotent stem cells. *J. of Controlled Release*, 2016, **235**, P. 222–235.
[54] Goenka S., Sant V., Sant S. Graphene-based nanomaterials for drug delivery and tissue engineering. *J. of Controlled Release*, 2014, **173**, P. 75–88.
[55] Teimouri M., Nia A.H., Abnous K., Eshghi H., Ramezani M. Graphene oxide–cationic polymer conjugates: Synthesis and application as gene delivery vectors. *Plasmid.*, 2016, **84–85**, P. 51–60.
[56] Hu H., Tang C., Yin C. Folate conjugated trimethyl chitosan/graphene oxide nanocomplexes as potential carriers for drug and gene delivery. *Mater. Lett.*, 2014, **125**, P. 82–85.
[57] Yin D., Li Y., Lin H., Guo B., Du Y., Li X., Jia H., Zhao X., Tang J., Zhang L. Functional graphene oxide as a plasmid-based Stat3 siRNA carrier inhibits mouse malignant melanoma growth *in vivo*. *Nanotechnology*, 2013, **24** (10), 105102.
[58] Zhi F., Dong H., Jia X., Guo W., Lu H., Yang Y., Ju H., Zhang X., Hu Y. Functionalized Graphene Oxide Mediated Adriamycin Delivery and miR-21 Gene Silencing to Overcome Tumor Multidrug Resistance In Vitro. *PLoS One*, 2013, **8** (3), e60034.
[59] Cheng F.-F., Chen W., Hu L.-H., Chen G., Miao H.-T., Li C., Zhu J.-J. Highly dispersible PEGylated graphene/Au composites as gene delivery vector and potential cancer therapeutic agent. *J. Mater. Chem. B*, 2013, **1** (38), 4956.
[60] Tripathi S.K., Goyal R., Gupta K.C., Kumar P. Functionalized graphene oxide mediated nucleic acid delivery. *Carbon N.Y.*, 2013, **51**, P. 224–235.
[61] He Y., Zhang L., Chen Z., Liang Y., Zhang Y., Bai Y., Zhang J., Li Y. Enhanced chemotherapy efficacy by co-delivery of shABCG2 and doxorubicin with a pH-responsive charge-reversible layered graphene oxide nanocomplex. *J. Mater. Chem. B*, 2015, **3** (31), P. 6462–6472.

[62] Yin F., Hu K., Chen Y., Yu M., Wang D., Wang Q., Yong K.-T., Lu F., Liang Y., Li Z. SiRNA Delivery with PEGylated Graphene Oxide Nanosheets for Combined Photothermal and Genetherapy for Pancreatic Cancer. *Theranostics*, 2017, **7** (5), P. 1133–1148.
[63] Feng L., Zhang S., Liu Z. Graphene based gene transfection. *Nanoscale*, 2011, **3** (3), 1252.
[64] Teng Y.D., Lavik E.B., Qu X., Park K.I., Ourednik J., Zurakowski D., Langer R., Snyder E.Y. Functional recovery following traumatic spinal cord injury mediated by a unique polymer scaffold seeded with neural stem cells. *Proceedings of the National Academy of Sciences*, 2002, **99** (5), P. 3024–3029.
[65] Solanki A., Chueng S.D., Yin P.T., Kappera R., Chhowalla M., Lee K. Axonal Alignment and Enhanced Neuronal Differentiation of Neural Stem Cells on Graphene? Nanoparticle Hybrid Structures. *Advanced Materials*, 2013, **25** (38), P. 5477–5482.
[66] Setia Budi H., Javed Ansari M., Abdalkareem Jasim S., Abdelbasset W.K., Bokov D., Fakri Mustafa Y., Najm M.A.A., Kazemnejadi M. Preparation of antibacterial Gel/PCL nanofibers reinforced by dicalcium phosphate-modified graphene oxide with control release of clindamycin for possible application in bone tissue engineering. *Inorg. Chem. Commun.*, 2022, **139**, 109336.
[67] Amiryaghoubi N., Fathi M., Barar J., Omidian H., Omidi Y. Recent advances in graphene-based polymer composite scaffolds for bone/cartilage tissue engineering. *J. Drug Deliv. Sci. Technol.*, 2022, **72**, 103360.
[68] Sharifi S., Ebrahimian-Hosseinabadi M., Dini G., Toghyani S. Magnesium-zinc-graphene oxide nanocomposite scaffolds for bone tissue engineering. *Arabian J. of Chemistry*, 2023, **16** (6), 104715.
[69] Ghosal K., Mondal P., Bera S., Ghosh S. Graphene family nanomaterials- opportunities and challenges in tissue engineering applications. *FlatChem*, 2021, **30**, 100315.
[70] Challa A.A., Saha N., Szewczyk P.K., Karbowniczek J.E., Stachewicz U., Ngwabebhoh F.A., Saha P. Graphene oxide produced from spent coffee grounds in electrospun cellulose acetate scaffolds for tissue engineering applications. *Mater Today Commun.*, 2023, **35**, 105974.
[71] Motiee E.-S., Karbasi S., Bidram E., Sheikholeslam M. Investigation of physical, mechanical and biological properties of polyhydroxybutyrate-chitosan/graphene oxide nanocomposite scaffolds for bone tissue engineering applications. *Int. J. Biol. Macromol.*, 2023, **247**, 125593.
[72] Babakhani A., Peighambardoust S.J., Olad A. Fabrication of magnetic nanocomposite scaffolds based on polyvinyl alcohol-chitosan containing hydroxyapatite and clay modified with graphene oxide: Evaluation of their properties for bone tissue engineering applications. *J. Mech. Behav. Biomed. Mater*, 2024, **150**, 106263.
[73] Amiryaghoubi N., Fathi M., Barar J., Omidian H., Omidi Y. Hybrid polymer-grafted graphene scaffolds for microvascular tissue engineering and regeneration. *Eur. Polym. J.*, 2023, **193**, 112095.
[74] Saravanan S., Sareen N., Abu-El-Rub E., Ashour H., Sequiera G.L., Ammar H.I., Gopinath V., Shamaa A.A., Sayed S.S.E., Moudgil M., Vadivelu J., Dhingra S. Graphene Oxide-Gold Nanosheets Containing Chitosan Scaffold Improves Ventricular Contractility and Function After Implantation into Infarcted Heart. *Sci. Rep.*, 2018, **8** (1), 15069.
[75] Park J., Kim B., Han J., Oh J., Park S., Ryu S., Jung S., Shin J.-Y., Lee B.S., Hong B.H., Choi D., Kim B.-S. Graphene Oxide Flakes as a Cellular Adhesive: Prevention of Reactive Oxygen Species Mediated Death of Implanted Cells for Cardiac Repair. *ACS Nano*, 2015, **9** (5), P. 4987–4999.
[76] Shin Y.C., Lee J.H., Jin L., Kim M.J., Kim Y.-J., Hyun J.K., Jung T.-G., Hong S.W., Han D.-W. Stimulated myoblast differentiation on graphene oxide-impregnated PLGA-collagen hybrid fibre matrices. *J. Nanobiotechnology*, 2015, **13** (1), 21.
[77] Chaudhuri B., Bhadra D., Moroni L., Pramanik K. Myoblast differentiation of human mesenchymal stem cells on graphene oxide and electrospun graphene oxide–polymer composite fibrous meshes: importance of graphene oxide conductivity and dielectric constant on their biocompatibility. *Biofabrication*, 2015, **7** (1), 015009.
[78] Shahmoradi S., Golzar H., Hashemi M., Mansouri V., Omidi M., Yazdian F., Yadegari A., Tayebi L. Optimizing the nanostructure of graphene oxide/silver/arginine for effective wound healing. *Nanotechnology*, 2018, **29** (47), 475101.
[79] Boga J.C., Miguel S.P., de Melo-Diogo D., Mendonça A.G., Louro R.O., Correia I.J. In vitro characterization of 3D printed scaffolds aimed at bone tissue regeneration. *Colloids Surf B Biointerfaces*, 2018, **165**, P. 207–218.
[80] Faghihi S., Karimi A., Jamadi M., Imani R., Salarian R. Graphene oxide/poly(acrylic acid)/gelatin nanocomposite hydrogel: Experimental and numerical validation of hyperelastic model. *Materials Science and Engineering: C*, 2014, **38**, P. 299–305.
[81] Liu H., Cheng J., Chen F., Bai D., Shao C., Wang J., Xi P., Zeng Z. Gelatin functionalized graphene oxide for mineralization of hydroxyapatite: biomimetic and in vitro evaluation. *Nanoscale*, 2014, **6** (10), 5315.
[82] Yu P., Bao R.-Y., Shi X.-J., Yang W., Yang M.-B. Self-assembled high-strength hydroxyapatite/graphene oxide/chitosan composite hydrogel for bone tissue engineering. *Carbohydr. Polym.*, 2017, **155**, P. 507–515.
[83] Wang L., Lu R., Hou J., Nan X., Xia Y., Guo Y., Meng K., Xu C., Wang X., Zhao B. Application of injectable silk fibroin/graphene oxide hydrogel combined with bone marrow mesenchymal stem cells in bone tissue engineering. *Colloids Surf A Physicochem. Eng. Asp.*, 2020, **604**, 125318.
[84] Qin H., Ji Y., Li G., Xu X., Zhang C., Zhong W., Xu S., Yin Y., Song J. MicroRNA-29b/graphene oxide–polyethyleneglycol–polyethylenimine complex incorporated within chitosan hydrogel promotes osteogenesis. *Front Chem.*, 2022, **10**.
[85] Khan M.R., Huang C., Ullah R., Ullah H., Qazi I.M., Nawaz T., Adnan M., Khan A., Su H., Ren L. Effects of Various Polymeric Films on the Pericarp Microstructure and Storability of Longan (cv. Shixia) Fruit Treated with Propyl Disulfide Essential Oil from the Neem (Azadirachta indica) Plant. *Polymers (Basel)*, 2022, **14** (3), 536.
[86] Xue B., Sheng H., Li Y., Li L., Di W., Xu Z., Ma L., Wang X., Jiang H., Qin M., Yan Z., Jiang Q., Liu J.-M., Wang W., Cao Y. Stretchable and self-healable hydrogel artificial skin. *Natl. Sci. Rev.*, 2022, **9** (7).
[87] Zhao, P., Zhang Y., Chen X., Xu C., Guo J., Deng M., Qu X., Huang P., Feng Z., Zhang J. Versatile Hydrogel Dressing with Skin Adaptiveness and Mild Photothermal Antibacterial Activity for Methicillin?Resistant Staphylococcus Aureus?Infected Dynamic Wound Healing. *Advanced Science*, 2023, **10** (11).
[88] Zhou J., Yang X., Liu W., Wang C., Shen Y., Zhang F., Zhu H., Sun H., Chen J., Lam J., Mikos A.G., Wang C. Injectable OPF/graphene oxide hydrogels provide mechanical support and enhance cell electrical signaling after implantation into myocardial infarct. *Theranostics*, 2018, **8** (12), P. 3317–3330.
[89] Yuan Z., Qin Q., Yuan M., Wang H., Li R. Development and novel design of clustery graphene oxide formed Conductive Silk hydrogel cell vesicle to repair and routine care of myocardial infarction: Investigation of its biological activity for cell delivery applications. *J. Drug Deliv. Sci. Technol.*, 2020, **60**, 102001.
[90] Chinemerem Nwobodo D., Ugwu M.C., Oliseloke Anie C., Al-Ouqaili M.T.S., Chinedu Ikem J., Victor Chigozie U., Saki M. Antibiotic resistance: The challenges and some emerging strategies for tackling a global menace. *J. Clin. Lab. Anal.*, 2022, **36** (9).
[91] Mitsunaga M., Ito K., Nishimura T., Miyata H., Miyakawa K., Morita T., Ryo A., Kobayashi H., Mizunoe Y., Iwase T. Antimicrobial strategy for targeted elimination of different microbes, including bacterial, fungal and viral pathogens. *Commun. Biol.*, 2022, **5** (1), 647.
[92] Kulakova I.I., Lisichkin G.V. Potential Directions in the Use of Graphene Nanomaterials in Pharmacology and Biomedicine (Review). *Pharm. Chem. J.*, 2022, **56** (1), P. 1–11.

[93] Bousiakou L.G., Qindeel R., Al-Dossary O.M., Kalkani H. Synthesis and characterization of graphene oxide (GO) sheets for pathogen inhibition: Escherichia coli, Staphylococcus aureus and Pseudomonas aeruginosa. *J. King Saud. Univ. Sci.*, 2022, **34** (4), 102002.
[94] Dan S., Bagheri H., Shahidizadeh A., Hashemipour H. Performance of graphene Oxide/SiO_2 Nanocomposite-based: Antibacterial Activity, dye and heavy metal removal. *Arabian J. of Chemistry*, 2023, **16** (2), 104450.
[95] Tariq M., Khan A.U., Rehman A.U., Ullah S., Jan A.U., Zakareya Khan Z.U.H., Muhammad N., Islam Z.U., Yuan Q. Green synthesis of Zno@GO nanocomposite and its' efficient antibacterial activity. *Photodiagnosis Photodyn. Ther.*, 2021, **35**, 102471.
[96] Bhatt S., Punetha V.D., Pathak R., Punetha M. Graphene in nanomedicine: A review on nano-bio factors and antibacterial activity. *Colloids Surf B Biointerfaces*, 2023, **226**, 113323.
[97] Abdollahzadeh S., Sayadi M.H., Shekari H. Synthesis of biodegradable antibacterial nanocomposite (metal–organic frameworks supported by chitosan and graphene oxide) with high stability and photocatalytic activities. *Inorg. Chem. Commun.*, 2023, **156**, 111302.
[98] Bentedlaouti K., Belouatek A., Kebaili N. Antibacterial and antioxidant activities of graphene and graphene oxide synthesis coated silver nanoparticules. *J. Cryst. Growth*, 2024, **627**, 127527.
[99] Khan A., Zaid M., Ameen F., Khan Mo.A., Kumar S., Al-Masri A.A., Islam M.A. Colossal antibacterial, antibiofilm and solar light-driven photocatalytic activity of nanoenhanced conjugate of bimetallic Ag-Zr nanoparticles with graphene oxide. *J. Mol. Struct.*, 2024, **1300**, 137223.
[100] Dwitya S.S., Hsueh Y.-H., Wang S.S.-S., Lin K.-S. Ultrafine nitrogen-doped graphene quantum dot structure and antibacterial activities against Bacillus subtilis 3610. *Mater. Chem. Phys.*, 2023, **295**, 127135.
[101] Avatefi Hemmat M., Asghari S., Bakhshesh M., Mahmoudifard M. Copper iodide decorated graphene oxide as a highly efficient antibacterial and antiviral nanocomposite. *Inorg. Chem. Commun.*, 2023, **156**, 111214.
[102] Fardinpour P., Ghafouri Taleghani H., Reza Zakerimehr M. Facile green synthesis of graphene oxide/copper oxide nanocomposites using ginger essential oil and its enhanced antibacterial properties. *Materials Science and Engineering: B*, 2024, **300**, 117100.
[103] Aissou T., Jann J., Faucheux N., Fortier L.-C., Braidy N., Veilleux J. Suspension plasma sprayed copper-graphene coatings for improved antibacterial properties. *Appl. Surf. Sci.*, 2023, **639**, 158204.
[104] Yang F., Huo D., Zhang J., Lin T., Zhang J., Tan S., Yang L. Fabrication of graphene oxide/copper synergistic antibacterial coating for medical titanium substrate. *J. Colloid Interface Sci.*, 2023, **638**, P. 1–13.
[105] Abdelhalim A.O.E., Galal A., Hussein M.Z., El Sayed I.E.-T. Graphene Functionalization by 1,6-Diaminohexane and Silver Nanoparticles for Water Disinfection. *J. Nanomater.*, 2016, **2016**, P. 1–7.
[106] Derakhshi M., Ashkarran A.A., Bahari A., Bonakdar S. Shape selective silver nanostructures decorated amine-functionalized graphene: A promising antibacterial platform. *Colloids Surf. A Physicochem. Eng. Asp.*, 2018, **545**, P. 101–109.
[107] Chen P., Ze R., Xia X., Zhang Z., Lu K., Wei L., Zhou B. Composite porphyrin-based conjugated microporous polymer/graphene oxide capable of photo-triggered combinational antibacterial therapy and wound healing. *Biomaterials Advances*, 2023, **154**, 213662.
[108] Wang Z., Liu G., Chen W., Zhang L., Qi Z., Bai G., Fan Y., Liu C., Xiao C., Li W., Chang Y., Liang G., Zhou Z., Yu P., Song Z., Ning C. Contribution of surface plasmonic resonance to enhanced photocatalytic antibacterial performance of graphene-based two-dimensional heterojunction. *Chemical Engineering J.*, 2023, **460**, 141720.
[109] Sun J., Liu X., Lyu C., Hu Y., Zou D., He Y.S., Lu J. Synergistic antibacterial effect of graphene-coated titanium loaded with levofloxacin. *Colloids Surf. B Biointerfaces*, 2021, **208**, 112090.
[110] Kumar S., Singh H., Feder-kubis J., Nguyen D.D. Recent advances in nanobiosensors for sustainable healthcare applications: A systematic literature review. *Environ. Res.*, 2023, **238** (P2), 117177.
[111] Arshad F., Nabi F., Iqbal S., Khan R.H. Applications of graphene-based electrochemical and optical biosensors in early detection of cancer biomarkers. *Colloids Surf. B Biointerfaces*, 2022, **212**, 112356.
[112] Oliveira M.E., Lopes B.V., Rossato J.H.H., Maron G.K., Gallo B.B., La Rosa A.B., Balboni R.D.C., Alves M.L.F., Ferreira M.R.A., da Silva Pinto L., Conceição F.R., Piva E., de Pereira C.M.P., Escote M.T., Carreño N.L.V. Electrochemical Biosensor Based on Laser-Induced Graphene for COVID-19 Diagnosing: Rapid and Low-Cost Detection of SARS-CoV-2 Biomarker Antibodies. *Surfaces*, 2022, **5** (1), P. 187–201.
[113] Bai Y., Xu T., Zhang X. Graphene-Based Biosensors for Detection of Biomarkers. *Micromachines*, 2020, **11** (1), 60.
[114] Peña-Bahamonde J., Nguyen H.N., Fanourakis S.K., Rodrigues D.F. Recent advances in graphene-based biosensor technology with applications in life sciences. *J. Nanobiotechnology*, 2018, **16** (1), P. 1–17.
[115] Sharifi M., Hasan A., Attar F., Taghizadeh A., Falahati M. Development of point-of-care nanobiosensors for breast cancers diagnosis. *Talanta*, 2020, **217**.
[116] Irkham I., Ibrahim A.U., Pwavodi P.C., Al-Turjman F., Hartati Y.W. Smart Graphene-Based Electrochemical Nanobiosensor for Clinical Diagnosis: Review. *Sensors (Basel)*, 2023, **23** (4).
[117] Achi F., Attar A.M., Ait Lahcen A. Electrochemical nanobiosensors for the detection of cancer biomarkers in real samples: Trends and challenges. *TrAC Trends in Analytical Chemistry*, 2023, 117423.
[118] Wu T., Shen J., Li Z., Xing F., Xin W., Wang Z., Liu G., Han X., Man Z., Fu S. Microfluidic-integrated graphene optical sensors for real-time and ultra-low flow velocity detection. *Appl. Surf. Sci.*, 2021, **539**, 148232.
[119] Mondal R., Dam P., Chakraborty J., Paret M.L., Kati A., Altuntas S., Sarkar R., Ghorai S., Gangopadhyay D., Mandal A.K., Husen A. Potential of nanobiosensor in sustainable agriculture: the state-of-art. *Heliyon*, , **8** (12), e12207.
[120] Bakhshpour M., Göktürk I., Gür S.D., Yilmaz F., Denizli A. Sensor Applications for Detection in Agricultural Products, Foods, and Water, in *Pesticides Bioremediation*, 2022, Springer International Publishing, Cham, P. 311–352.
[121] Hernández R., Vallés C., Benito A.M., Maser W.K., Xavier Rius F., Riu J. Graphene-based potentiometric biosensor for the immediate detection of living bacteria. *Biosens. Bioelectron.*, 2014, **54**, P. 553–557.
[122] Cai Y., Chen D., Chen Y., Li T., Wang L., Jiang J., Guo Z., Jaffrezic-Renault N., Zhang Z., Huang S. An electrochemical biosensor based on graphene intercalated functionalized black phosphorus/gold nanoparticles nanocomposites for the detection of bacterial enzyme. *Microchemical J.*, 2023, **193**, 109255.
[123] Yang X., Yin Z.Z., Zheng G., Zhou M., Zhang H., Li J., Cai W., Kong Y. Molecularly imprinted miniature electrochemical biosensor for SARS-CoV-2 spike protein based on Au nanoparticles and reduced graphene oxide modified acupuncture needle. *Bioelectrochemistry*, 2023, **151**, 108375.
[124] Gao J., Wang C., Chu Y., Han Y., Gao Y., Wang Y., Wang C., Liu H., Han L., Zhang Y. Graphene oxide-graphene Van der Waals heterostructure transistor biosensor for SARS-CoV-2 protein detection. *Talanta*, 2022, **240**, 123197.
[125] Malla P., Liu C.H., Wu W.C., Kabinsing P., Sreearunothai P. Synthesis and characterization of Au-decorated graphene oxide nanocomposite for magneto-electrochemical detection of SARS-CoV-2 nucleocapsid gene. *Talanta*, 2023, **262**, 124701.
[126] Lahcen A.A., Rauf S., Aljedaibi A., de Oliveira Filho J.I., Beduk T., Mani V., Alshareef H.N., Salama K.N. Laser-scribed graphene sensor based on gold nanostructures and molecularly imprinted polymers: Application for Her-2 cancer biomarker detection. *Sens Actuators B Chem.*, 2021, **347**, 130556.

[127] Wu T.Z., Jian C.R., Govindasamy M., Li Y.C., Lin Y.T., Su C.Y., Samukawa S., Huang C.H. Crumpled graphene induced by commercial Heat-Shrinkable material for chemiresistive biosensors toward cancer biomarker detection. *Microchemical J.*, 2023, **195**, 109469.

[128] Yan M., Fu L. ling Feng H. chao Namadchian M. Application of Ag nanoparticles decorated on graphene nanosheets for electrochemical sensing of CEA as an important cancer biomarker. *Environ. Res.*, 2023, **239**, 117363.

[129] Rajaji U., Muthumariyappan A., Chen S.M., Chen T.W., Ramalingam R.J. A novel electrochemical sensor for the detection of oxidative stress and cancer biomarker (4-nitroquinoline N-oxide) based on iron nitride nanoparticles with multilayer reduced graphene nanosheets modified electrode. *Sens Actuators B Chem.*, 2019, **291**, P. 120–129.

[130] Rauf S., Mishra G.K., Azhar J., Mishra R.K., Goud K.Y., Nawaz M.A.H., Marty J.L., Hayat A. Carboxylic group riched graphene oxide based disposable electrochemical immunosensor for cancer biomarker detection. *Anal. Biochem.*, 2018, **545**, P. 13–19.

[131] Kumar S., Gupta N., Malhotra B.D. Ultrasensitive biosensing platform based on yttria doped zirconia-reduced graphene oxide nanocomposite for detection of salivary oral cancer biomarker. *Bioelectrochemistry*, 2021, **140**, 107799.

[132] Singh V.K., Kumar S., Pandey S.K., Srivastava S., Mishra M., Gupta G., Malhotra B.D., Tiwari R.S., Srivastava A. Fabrication of sensitive bioelectrode based on atomically thin CVD grown graphene for cancer biomarker detection. *Biosens. Bioelectron.*, 2018, **105**, P. 173–181.

[133] Sadeghi M., Kashanian S., Naghib S.M., Haghiralsadat F., Tofighi D. An Efficient Electrochemical Biosensor Based on Pencil Graphite Electrode Mediated by 2D Functionalized Graphene Oxide to Detect HER2 Breast Cancer Biomarker. *Int. J. Electrochem. Sci.*, 2022, **17** (4), 220459.

[134] Chen T.W., Rajaji U., Chen S.M., Li Y.L., Ramalingam R.J. Ultrasound-assisted synthesis of α-MnS (alabandite) nanoparticles decorated reduced graphene oxide hybrids: Enhanced electrocatalyst for electrochemical detection of Parkinson's disease biomarker. *Ultrason. Sonochem.*, 2019, **56**, P. 378–385.

Submitted 21 June 2024; revised 8 October 2024; accepted 7 November 2024

Information about the authors:

Konstantin N. Semenov – Pavlov First St. Petersburg State Medical University, 6–8 L'va Tolstogo Street, St. Petersburg, 197022, Russia; St. Petersburg State University, 7–9 Universitetskaia Embankment, St. Petersburg, 199034, Russia; A. M. Granov Russian Research Centre for Radiology and Surgical Technologies, 70 Leningradskaia Street, St. Petersburg, 197758, Russia; ORCID ; knsemenov@gmail.com

Sergei V. Ageev – Pavlov First St. Petersburg State Medical University, 6–8 L'va Tolstogo Street, St. Petersburg, 197022, Russia; St. Petersburg State University, 7–9 Universitetskaia Embankment, St. Petersburg, 199034, Russia; ORCID ; ageev.sergey06@gmail.com

Olga S. Shemchuk – Pavlov First St. Petersburg State Medical University, 6–8 L'va Tolstogo Street, St. Petersburg, 197022, Russia; A. M. Granov Russian Research Centre for Radiology and Surgical Technologies, 70 Leningradskaia Street, St. Petersburg, 197758, Russia; ORCID ; olja.shemchuk17@gmail.com

Gleb O. Iurev – Pavlov First St. Petersburg State Medical University, 6–8 L'va Tolstogo Street, St. Petersburg, 197022, Russia; A. M. Granov Russian Research Centre for Radiology and Surgical Technologies, 70 Leningradskaia Street, St. Petersburg, 197758, Russia; ORCID ;

Abdelsattar O. E. Abdelhalim – Environmental Research Department, National Centre for Social and Criminological Research (NCSCR), Giza 11561, Egypt; ORCID ; abdelsattarosama@yahoo.com

Igor V. Murin – St. Petersburg State University, 7–9 Universitetskaia Embankment, St. Petersburg, 199034, Russia; ORCID ; igormurin@mail.ru

Pavel K. Kozhukhov – Pavlov First St. Petersburg State Medical University, 6–8 L'va Tolstogo Street, St. Petersburg, 197022, Russia; ORCID ; kozhukhovpk@yandex.ru

Anastasia V. Penkova – St. Petersburg State University, 7–9 Universitetskaia Embankment, St. Petersburg, 199034, Russia; ORCID ;

Dmitriy N. Maystrenko – A. M. Granov Russian Research Centre for Radiology and Surgical Technologies, 70 Leningradskaia Street, St. Petersburg, 197758, Russia; ORCID ; may68@mail.ru

Oleg E. Molchanov – A. M. Granov Russian Research Centre for Radiology and Surgical Technologies, 70 Leningradskaia Street, St. Petersburg, 197758, Russia; ORCID ; molchanovo@mail.ru

Vladimir V. Sharoyko – Pavlov First St. Petersburg State Medical University, 6–8 L'va Tolstogo Street, St. Petersburg, 197022, Russia; St. Petersburg State University, 7–9 Universitetskaia Embankment, St. Petersburg, 199034, Russia; A. M. Granov Russian Research Centre for Radiology and Surgical Technologies, 70 Leningradskaia Street, St. Petersburg, 197758, Russia; ORCID ; sharoyko@gmail.com

Conflict of interest: the authors declare no conflict of interest.